Failure Mechanisms of a SiC Particles/2024Al Composite under Dynamic Loading

Y.X. Lu (a, b), X.M. Meng (a, b), C.S. Lee (a), R.K.Y. Li (a),
and C.G. Huang (a, c)

(a) *Department of Physics and Materials Science, City University of Hong Kong,*
Tat Chee Avenue, Hong Kong

(b) *Institute of Metal Research, Chinese Academy of Sciences, Shenyang 110015,*
People's Republic of China

(c) *Institute of Mechanics, Chinese Academy of Sciences, Beijing,*
People's Republic of China

Dynamic mechanical response of a 20 vol% silicon carbide particles (SiCp) reinforced 2024 Al composite prepared by powder metallurgy techniques were studied with a split Hopkinson bar. The fracture mechanisms and the deformation microstructure were examined with Scanning Electron Microscopy (SEM) and Transmission Electron Microscopy (TEM). The present results indicate that the composite has a strong SiC–Al interfacial bonding; failure of the material is mainly caused by fracture of SiC particles and tearing failure of the SiC–Al interface. This failure by interface tearing with adhesion of an aluminium layer on SiC particles on the fracture surfaces has not been reported in SiC particle–reinforced aluminium composites. High-resolution transmission electron microscopy studies showed that many of the SiC–Al interfaces have coincident site lattice structures, which are considered to make a significant contribution to the strong interfacial bonding.

1. Introduction

SiC reinforced aluminium composites have various superior properties including high elastic moduli, high yield strength and wear resistance. These composites can also be processed by conventional metal processing techniques at reasonable cost. Thus, SiC/Al composites have good potential for large-scale applications in various structural components. In order to improve their fracture resistance, failure mechanisms of these composites have been extensively studied in the past decade [1 to 6]. These works suggested that the failure mechanisms are related to various factors including size, volume fraction and distribution of the SiC phase, chemical composition and heat treatment of the matrix as well as processing history of the composites. Based on TEM observations, Nutt and Duva [7] suggested that failure of SiC whisker-reinforced aluminium composites is mainly initiated by nucleation and growth of voids and cracks at the corners of the whiskers where the stress concentration is high. These cracks would then propagate along the SiC/Al interface and lead to the final fracture. While this failure mechanism for SiC whisker-reinforced aluminium composites is widely accepted, there is no single generally agreed failure mechanism for SiC particle-reinforced aluminium composites. Most commonly reported failure mechanisms are ductile failure of the matrix [3, 8],

fracture of the reinforcement particles [9 to 11] and interfacial debonding [10, 11]. Lloyd et al. [12] attributed the three types of failure to the relative strength of the matrix, reinforcement phase and their interfacial bonding. When the SiC–Al interfacial bonding is weak, the composite will fail by interfacial debonding. In composites with good interfacial bonding but low matrix strength, failure of the composites will be initiated by ductile yielding of the matrix. When strengths of both the matrix and the interfacial bonding are high, the composite will fail by brittle fracture of the reinforcement phase.

While substantial works have been done on the fracture mechanisms of SiCp/Al composites under static loading, there are relative few works on the fracture mechanism under dynamic loading [14, 15]. In particular, the present understanding on the relationships between the mechanical properties, fracture mechanisms and microstructure are still far from adequate. These understandings are obviously needed for large-scale industrial applications of the materials. In the present work, the deformation microstructure and fracture mechanisms of a 20 vol% 3.5 μm SiCp/2024Al composite deformed under dynamic loading conditions were studied.

2. Materials and Experimental

The SiCp/2024Al composite used in the present paper was fabricated by a powder metallurgy process using 2024Al powder of 280 grits and SiC particles with an average grain size of 3.5 μm. The mixed powder with a SiC volume fraction of 20% was compacted by hot compression under vacuum. The compacted powder was then extruded at 450 °C to rods of 1.2 cm diameter with an extrusion ratio of 40:1. The composite was then solution treated at 500 °C for 1 h followed by water quenching and subsequently ageing at 170 °C for a duration of 6 h (T6 treatment). The microstructure of the as-prepared composite is shown in Fig. 1, which indicates that SiC particles are evenly distributed and there is no observable defect. Tensile samples of 0.32 cm diameter × 1 cm gauge length and compression samples of 0.8 cm diameter × 0.6 cm height
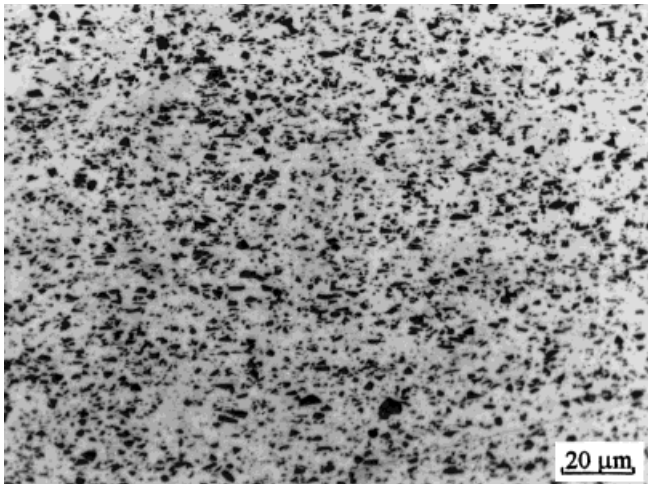

Fig. 1. Optical micrograph of the as-prepared 20 vol% 3.5 μm SiCp/2024Al composite

were machined from the rod along the extrusion direction. Dynamic tensile and compression tests were carried out with a split Hopkinson bar at a strain rate of 10^3 s^{-1}. The working principle and set-up of a Hopkinson bar can be found in the literature [16]. TEM specimens were made from thin slices of about 150 μm cut parallel to the extrusion direction. The slices were mechanically ground to 70 μm, dimpled to 25 μm and finally ion thinned at 4 kV with an incident angle of 11°. TEM specimens were examined with either a Philips CM20 or a JEOL 2000EX operated at 200 kV. Fracture surfaces of the tensile samples were observed with a SEM. The microstructure and the distribution of SiC particles were observed with an optical microscope.

3. Results and Discussion

Dynamic stress–strain curves of the composite tested in tension and in compression at a strain rate of 10^3 s^{-1} are shown in Fig. 2. Work hardening can be observed in the initial stage of the plastic deformation. The flow stresses reach their saturation values after about 5% strain. The tensile flow stress is higher than the compressive flow stress at all strains. This asymmetry of the tensile and compressive strength is due to the internal residual stresses, originating in the difference in thermal expansion coefficient of the matrix and SiC particles, generated during the production process of the composite [13].

The tensile fracture surface shows features of brittle fracture at a relatively macroscopic scale (Fig. 3). However, in a microscopic view, dimples showing ductile shearing can also be seen. Dimples observed are of two different size ranges. The large and the small dimples have sizes similar to those of the SiC particles and precipitated phases (about 1 μm size), respectively. SiC particles found on the fracture surface are of two different types of feature. The first type shows a smooth and flat fracture surface along the cleavage planes of SiC. As SiC has several low index cleavage planes, the fracture
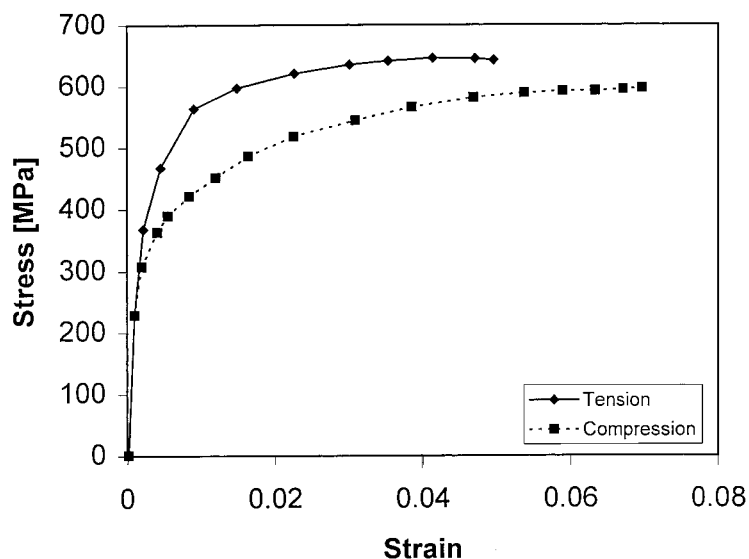

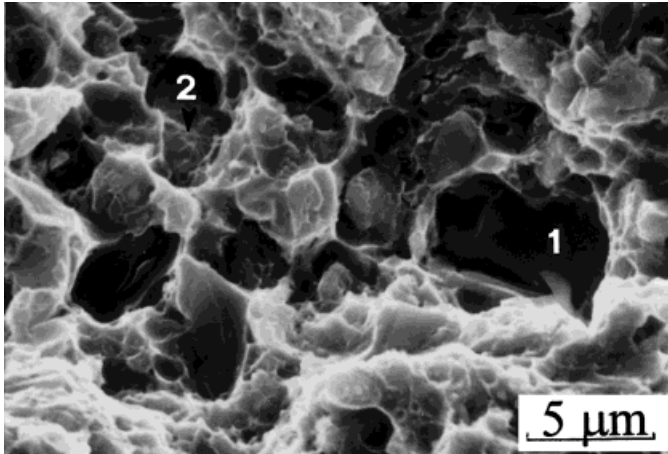Fig. 2. Stress–strain response of the composite at a strain rate of 10^3 s^{-1}

Fig. 3. Tensile fracture surface of the SiCp/2024Al composite

of SiC particles can proceed with cleavage along several planes simultaneously and gives rise to secondary cracks (marker 1 in Fig. 3). Some SiC particles on the fracture surface show a ductile tearing failure along the SiC–Al interface. This type of failure is different from the commonly observed interfacial debonding which would give rise to a much smoother fracture surface. Marker 2 in Fig. 3 shows a SiC particle adhering with ridges originated from tearing of the aluminium matrix. This was also verified by EDX analysis which showed that the aluminium content at marker 2 is much higher than that
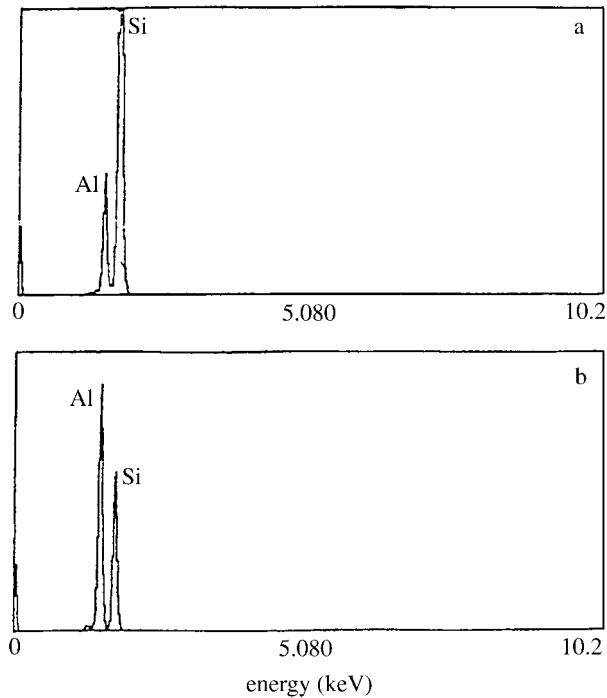

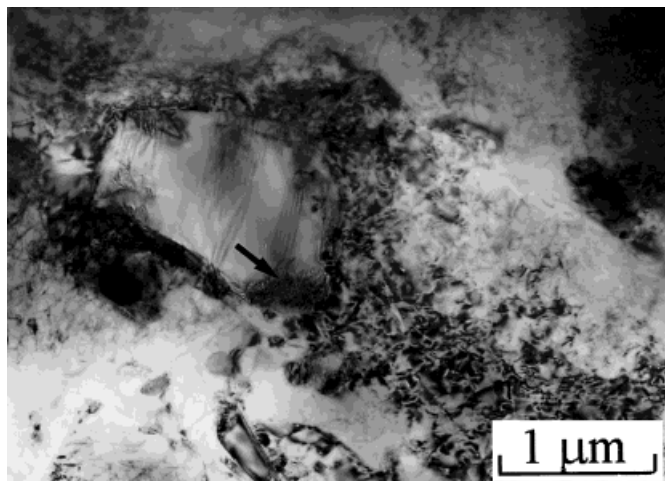Fig. 4. EDX spectra taken at a) marker 1 and b) marker 2 of the sample as shown in Fig. 3

Fig. 5. A TEM micrograph of the SiCp/2024Al composite after dynamic loading showing damages in the microstructure

at marker 1 (Fig. 4). This tearing failure near the SiCp/Al interface is similar to the corresponding observation in SiC whisker-reinforced Al composite [17]. However, to the authors' knowledge, it has not been reported in SiC particles reinforced aluminium composites. The tearing failure indicates that the composite used here has a high SiC–Al interfacial bonding strength.

TEM observations of the dynamically loaded samples show that various forms of defects were accumulated in the SiC particles. In addition to stacking faults, locations with high stress concentration, such as sharp corners of the SiC particles, were often fractured (Fig. 5). The dislocation density increased tremendously in both the interface and the matrix regions. Fracture of SiC was also observed with the cracks usually initiated from locations of high stress concentrations such as stacking faults or corners of the SiC particles (Fig. 6). Tearing failure found in the fracture surface (Fig. 3) and adhe-
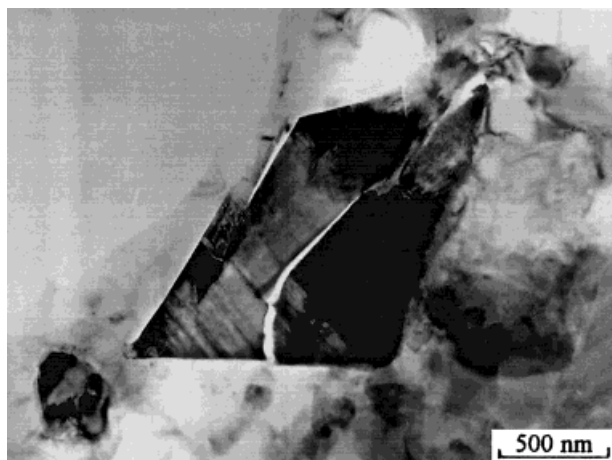

Fig. 6. A TEM micrograph showing cracking of a SiC particle after dynamic loading

Fig. 7. A TEM micrograph show-ing tearing of an Al–SiC interface

sion of aluminium to the SiC particle (indicated by an arrow) can also be observed in Fig. 7.

High-resolution TEM studies of the SiC–Al interface show that many of the SiC particles have coincident lattice sites with the matrix along the interface. Fig. 8 shows one of these interfaces (marked by double arrows), where the orientation relationship $[110]_{Al} \parallel [\bar{2}110]_{SiC}$, $(1\bar{1}1)_{Al} \parallel (0006)_{SiC}$ was observed (there is a small angle, about $2°$, between the Al $(1\bar{1}1)$ and the SiC (0006) planes). It can be seen that the interface is
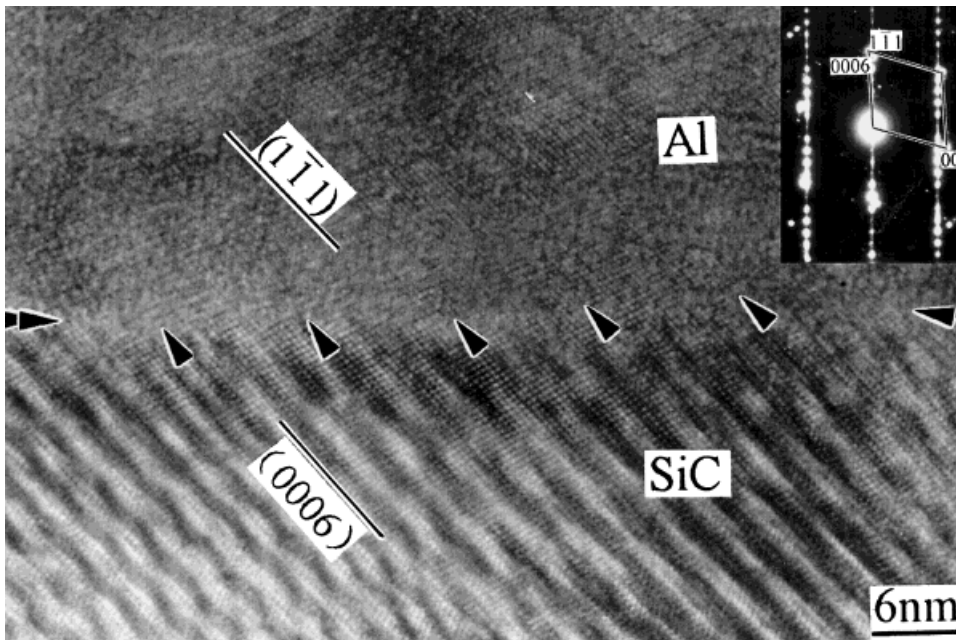

Fig. 8. A high-resolution TEM micrograph showing a coincident site lattice relationship in an Al–SiC interface. Selected area electron diffraction pattern from the interface is shown in the inset

smooth with some mismatch dislocations (marked by single arrows) due to the different spacings of the Al ($\bar{1}$11) and the SiC (0006) planes (0.234 and 0.251 nm, respectively). The high interfacial bonding strength in the present composite can be attributed to these interfaces with coincident site lattice. More systematic high-resolution TEM work on this issue is under way to fully characterize the interfaces in the present composite.

4. Conclusions

Failure mechanisms of a 20 vol% 3.5 μm SiCp/2024Al under dynamic loading condition were studied by SEM and TEM analysis. The present results indicated that the composite fails by tearing of the SiC–Al interface, which has not been reported in SiC particles reinforced aluminium matrix composites. This failure mechanism is attributed to the high interfacial bonding strength between the aluminium matrix and the SiC particles. The high interfacial strength can, in turn, be explained by the observation that many of the Al–SiC boundaries have coincident site lattice relationships.

References

[1] A.P. Divecha, S.G. Fishman, and S.D. Karmaker, J. Metals **33**, 12 (1981).
[2] D.L. McDonels, Metals Trans. **16A**, 1105 (1985).
[3] C.P. You, A.W. Thompson, and I.M. Bernstein, Scripta Metall. **21**, 181 (1987).
[4] D.J. Lloyd, Acta Metall. et Mater. **39**, 59 (1991).
[5] J.C. Lee and K.N. Subramanian, J. Mater. Sci. **27**, 5453 (1992).
[6] B. Wang, G.M. Janowski, and B.R. Patterson, Metals Trans. **16A**, 2457 (1995).
[7] S.R. Nutt and J.M. Duva, Scripta Metall. **20**, 1055 (1986).
[8] R.J. Arsenault, N. Shi, C.R. Feng, and L. Wang, Mater. Sci. Engng. A **131**, 56 (1991).
[9] J. Lorca, A. Martin, J. Ruiz, and M. Elices, Metals Trans. **24A**, 1575 (1993).
[10] J.J. Lewandowaki, C. Liu, and W. H. Hunt, Mater. Sci. Engng. A **107**, 241 (1989).
[11] P. Mummery and B. Derby, Mater. Sci. Engng. A **135**, 221 (1991).
[12] D.J. Lloyd, H.P. Lagace, and A.D. McLeod, Proc. ICCI-III, Ed. H. Ishinda, Elsevier Publ. Co., Amsterdam 1990 (p. 359).
[13] S.F. Corbin and D.S. Wilkinson, Acta Metall. et Mater. **42**, 1319 (1994).
[14] R.U. Vaidya, S.G. Song, and A.K. Zurek, Phil. Mag. **A70**, 819 (1994).
[15] R.U. Vaidya and A.K. Zurek, J. Mater. Sci. **30**, 2541 (1995).
[16] P.S. Follansbee, Metals Handbook, 9th ed., Vol. 8, ASM, Metals Park, Ohio 1985 (p. 190).
[17] J.G. Nieh, R.A. Rainen, and D.J. Chellman, Proc. ICCM5, San Diego, Eds. W.C. Harrigan, Jr. Strife, and A.K. Dhingra, TMS-AIME 1985 (p. 843).